Pain Medicine

Pain Medicine 2013; 14: 895–915
Wiley Periodicals, Inc.

MUSCULOSKELETAL SECTION

Original Research Article

Excessive Peptidergic Sensory Innervation of Cutaneous Arteriole–Venule Shunts (AVS) in the Palmar Glabrous Skin of Fibromyalgia Patients: Implications for Widespread Deep Tissue Pain and Fatigue

Phillip J. Albrecht, PhD,*,† Quanzhi Hou, MD PhD,*,† Charles E. Argoff, MD,‡ James R. Storey, MD,§ James P. Wymer, MD PhD,‡ and Frank L. Rice, PhD*,†

*Integrated Tissue Dynamics, LLC, Rensselaer, New York;

†Center for Neuropharmacology & Neuroscience and

‡Department of Neurology, Albany Medical College, Albany, New York;

§Upstate Clinical Research, LLC, Albany, New York, USA

Reprint requests to: Phillip J. Albrecht, PhD, Integrated Tissue Dynamics, LLC, 7 University Place, Rensselaer, NY 12144, USA. Tel: 866-610-7581; Fax: 518-262-5799; E-mail: philalbrecht@Intidyn.com; albrecp@mail.amc.edu.

The authors each declare no conflicts of interest associated with this research.

Correction made after online publication May 20, 2013: the author affiliations have been updated.

Abstract

Objective. To determine if peripheral neuropathology exists among the innervation of cutaneous arterioles and arteriole–venule shunts (AVS) in fibromyalgia (FM) patients.

Setting. Cutaneous arterioles and AVS receive a convergence of vasoconstrictive sympathetic innervation, and vasodilatory small-fiber sensory innervation. Given our previous findings of peripheral pathologies in chronic pain conditions, we hypothesized that this vascular location may be a potential site of pathology and/or serotonergic and norepinephrine reuptake inhibitors (SNRI) drug action.

Subjects. Twenty-four female FM patients and nine female healthy control subjects were enrolled for study, with 14 additional female control subjects included from previous studies. AVS were identified in hypothenar skin biopsies from 18/24 FM patient and 14/23 control subjects.

Methods. Multimolecular immunocytochemistry to assess different types of cutaneous innervation in 3 mm skin biopsies from glabrous hypothenar and trapezius regions.

Results. AVS had significantly increased innervation among FM patients. The excessive innervation consisted of a greater proportion of vasodilatory sensory fibers, compared with vasoconstrictive sympathetic fibers. In contrast, sensory and sympathetic innervation to arterioles remained normal. Importantly, the sensory fibers express α2C receptors, indicating that the sympathetic innervation exerts an inhibitory modulation of sensory activity.

Conclusions. The excessive sensory innervation to the glabrous skin AVS is a likely source of severe pain and tenderness in the hands of FM patients. Importantly, glabrous AVS regulate blood flow to the skin in humans for thermoregulation and to other tissues such as skeletal muscle during periods of increased metabolic demand. Therefore, blood flow dysregulation as a result of excessive innervation to AVS would likely contribute to the widespread deep pain and fatigue of FM. SNRI compounds may provide partial therapeutic benefit by enhancing the impact of sympathetically mediated inhibitory modulation of the excess sensory innervation.

Key Words. Cutaneous Innervation; Vasculature; Neuropathic Pain; Inflammation; Blood Flow

Introduction

Fibromyalgia (FM) is a common chronic widespread pain condition, afflicting 2–5% of the US population, with females being affected at well over twice the rate of males [1–3]. FM is a complex multifaceted disorder characterized by chronic widespread pain, allodynia, hyperalgesia, sensory sensitivities (visual, auditory), severe fatigue, sleeplessness, cognitive dysfunction, and endocrine abnormalities [4–7]. Disease modulators include psychologic and biologic stressors, diet, and genetic predispositions involving serotonin, dopamine, and/or norepinephrine/noradrenaline (NA) [1–2,8–9]. Current Food and Drug Administration (FDA)-approved treatments include serotonergic and norepinephrine reuptake inhibitors (SNRI), and a voltage-gated calcium channel subunit (alpha 2-delta) ligand, pregabalin. However, at best, these compounds provide temporary partial relief in only a portion of FM patients, and have dose limiting side effects [7,10–12].

The prevailing hypothesis of FM primarily postulates a sensitization of pain pathways in the central nervous system (CNS) accompanied by evidence of increased excitatory neurotransmitters and inflammatory cytokines in the cerebrospinal fluid (CSF) [5,13–17]. The source and maintenance of the CNS sensitization is unknown. To date, a peripheral nervous system (PNS) and/or target cell pathology has not been identified in FM patients, although evidence of small fiber neuropathy and cutaneous compartment pathologies have been detected in skin biopsies among several other chronic pain conditions [18–26]. Increasing evidence indicates that the excessive fatigue and widespread deep pain associated with FM is caused by peripheral tissue ischemia and hyperactivation of deep tissue nociceptors by anaerobic metabolites and inflammatory cytokines, a process that would drive and maintain CNS sensitization [1,27–29]. The source of the ischemia is assumed to arise from excessive sympathetically mediated vasoconstriction, which can also be exacerbated by stress [9,30–33].

Diagnosis of FM includes hypersensitivity to pressure applied to at least 11 out of 18 specific tender points, although more recent guidelines have placed less emphasis on tender point counts [34–35]. FM pain is widespread with mechanical allodynia, thermal sensitivity, and especially tenderness over most areas of the body. This includes the hands, which are not a diagnostic FM tender point site specifically, but have been used for extensive testing of pain thresholds and blood flow in FM patients [29,36–39]. Mechanical allodynia in response to pressure occurs rapidly as a “first pain” perception in most FM patients. Tests using heat stimulation demonstrate that heat hyperalgesia occurs as a delayed “second pain” response, forming the rationale for postulating a “windup” mechanism contributing to central sensitization [17,38,40]. However, cold conditions particularly aggravate FM pain and vasospasms [41], and cold dysesthesia and hyperalgesia occur more frequently in FM subjects, whereas heat hyperalgesia typically occurs without dysesthesia and only as a subset among those with cold hyperalgesia [36–37,42].

Although SNRI are mostly assumed to act on CNS mechanisms, our integrated multimolecular immunocytochemical analyses of cutaneous innervation in mammals ranging from rodents to primates, including humans, has documented that arterioles and arteriole–venule shunts (AVS) located deep in the dermis of glabrous skin are innervated by a convergence of dense sympathetic and sensory innervation that could be a peripheral target of SNRI [19,43–47]. In particular, the arterioles and AVS have a well-known, dense noradrenergic sympathetic innervation, whose role in vasoconstriction has been extensively researched, but also a lesser known, dense sensory innervation composed of several varieties of immunochemically distinct C and Aδ fibers.

We have previously hypothesized a functional role in chronic pain conditions of small-caliber sensory innervation to the cutaneous vasculature [19,43,45]. However, although nearly all sensory innervation to cutaneous vasculature contains substance P (SP) and calcitonin gene-related peptide (CGRP), which are potent vasodilators and are implicated in inflammatory pain mechanisms [48–53], this topic has received only little research attention. Thus, the sensory innervation likely plays a role in vascular-related sensory feedback to regulate sympathetic activity, but may also be implicated in a direct effector role in vasodilation and potential inflammation among FM patients [48–50,52,54–55]. Our previous multimolecular assessments demonstrated that the sensory fibers express the α2C receptor, indicating that the sympathetic innervation may exert a local inhibitory effect on the sensory activity [56–58]. We recently documented that this innervation may also contribute to a variety of conscious tactile sensations [43], but it undoubtedly works in concert with the sympathetic innervation for purposes of vasoregulation, especially the important thermoregulatory function of the glabrous skin in humans. Given the extreme sensitivity to cold conditions and stress, the deep pain sensation of FM patients, and the convergence and immunochemical properties of the sensory and sympathetic innervation, which could be a therapeutic target of SNRI, we hypothesized that FM patients might manifest a pathology involving the innervation to the cutaneous arterioles and AVS located deep in the dermis.

In order to assess the neurochemical and morphological characteristics of cutaneous innervation in FM compared with control subjects, we conducted multimolecular immunofluorescence analyses of 3 mm skin biopsies taken from the diagnostic trapezius tender point location and from the glabrous hypothenar skin where there is a high concentration of AVS [19,43,45,47]. Skin biopsies were collected from 24 female FM-diagnosed patients and 23 age-matched female control subjects. Only females were studied here based on the increased incidence of FM [3,8], which may be due to gender-related differences in vascular innervation [59–61]. We discovered excessive innervation of AVS in the palmar hypothenar skin of

the FM patients which was skewed toward an over-representation of peptidergic sensory innervation and an underrepresentation of NA sympathetic innervation. This AVS neurovascular pathology is consistent with FM symptoms of pain and tenderness, exacerbation of these symptoms by cold conditions, and the potential beneficial effects of SNRI agents. Moreover, this pathology may have wide-ranging implications impacting blood flow throughout the body which may contribute to ischemia and widespread symptoms of deep tissue pain and fatigue in FM [2,30].

Materials and Methods

The research protocol was approved by the Albany Medical Center Institutional Review Board (IRB), and all subjects gave written informed consent. All subjects were administered a medical evaluation to verify the absence of exclusionary diseases and signed appropriate IRB-approved consent prior to enrollment in the study. Skin biopsy collection was performed using established procedures and appropriate monitoring. No adverse events or serious adverse events attributed to the testing or biopsy procedures were documented for this study.

Study Design

This investigation was performed to assess cutaneous pathology and the effect of treatment on patients diagnosed with FM. The reported data are compiled from two cohorts, FM patient and control subjects, as described in Table 1. Cohort 1 consisted of 24 female adults diagnosed with FM based from the 1990 American College of Rheumatology (ACR) criteria, including widespread pain present for at least 3 months, pain in at least 11 of 18 specific tender point sites, and 22/24 had scores greater than 40 on the 100-point visual analog scale (VAS) [6,34]. After eligibility determination and informed consent, FM subjects underwent a washout of excluded (FM specific) medications and a 1-week baseline. Cohort 2 was composed of 23 age- and gender-matched control subjects, 9 enrolled for this study and 14 additional gender-matched control subject hypothenar biopsies from other ongoing IRB-approved studies. Comorbidities known to produce muscle pain, unstable medical conditions, and severe or uncontrolled depression were exclusion criteria for each group. Each enrolled subject was evaluated by standardized pain questionnaires, general and neurologic exam, tender point survey, and computerized quantitative sensory testing (QST) (Medoc, Durham, NC, USA). The QST was conducted on the dominate trapezius tender point site, a common location for intense FM pain. The full unblinding of the QST data is awaiting completion of the second portion of the ongoing study (FM response to medication).

Tissue

Immediately following the clinical assessments, a single 3 mm skin punch biopsy was collected under local lidocaine anesthetic from two distinct locations: 1) the trapezius thoracic tender point site utilized for QST testing, and 2) the palmar hypothenar glabrous skin compartment (halfway between proximal to distal extent of the compartment and about 1 cm from the medial margin). This pair of skin biopsies (one trapezius, one hypothenar) was collected from all 24 FM patients and the nine healthy controls specifically enrolled for this study. Only a hypothenar biopsy was collected under identical procedures from the additional 14 control subjects. The hypothenar biopsy site has a high probability of sampling cutaneous vasculature, including specifically AVS [18,43,62]. This skin biopsy location has been utilized routinely by Integrated Tissue Dynamics, LLC (Intidyn, Rensselaer, NY, USA) as part of an integrated multimolecular Chemomorphometric Analysis (CMA) platform, directed at profiling a wide variety of C, Aδ, and Aβ axon endings and terminal cell compartments [19,43,45,62]. A rich variety of large and small-caliber sensory endings and vascular structures are located within the hypothenar region, whereas these are sparse in back skin and rarely found in 3 mm biopsies obtained from that location. Immediately after removal, the biopsies were fixed by immersion in 4% paraformaldehyde (in 0.1 M phosphate-buffered saline; pH 7.4) for 4 hours at 4°C, then rinsed and stored in PBS at 4°C until processing. Biopsies were then cryoprotected overnight in 30% sucrose in PBS, frozen, and cryostat sectioned at 14 μm thickness perpendicular to the epidermal surface. The sections were thaw mounted in serial order, alternating across at least 20 slides such that each slide contained numerous sections from equally spaced intervals throughout the biopsy.

Immunochemistry

Biopsy specimen were processed following established protocols for integrated multimolecular immunofluorescence assessments [18,24,26,43,62] and were evaluated utilizing the CMA platform developed by Intidyn. This procedure enables the use of a wide variety of immunolabel (IL) combinations designed to elucidate different functional and morphological varieties of cutaneous innervation. Based on our previous research, we had identified that arterioles and AVS are innervated by four major subtypes, all of which express immunolabeling for the pan-neuronal enzyme protein gene product (PGP)9.5:

1. Unmyelinated peptidergic C fibers (CGRP-positive/neurofilament [NF]-negative) that are immunoreactive for CGRP and SP but lack immunoreactivity for 200 kD NF protein, myelin basic protein (MBP), neuropeptide Y (NPY), and tyrosine hydroxylase (TH). The CGRP-positive/NF-negative peptidergic C fibers are normally the vast majority of the vascular sensory innervation
2. Lightly myelinated peptidergic Aδ fibers (CGRP-positive/NF-positive) that are immunoreactive for NF, MBP, and CGRP, but not for NPY and TH.
3. Lightly myelinated nonpeptidergic Aδ fibers (CGRP-negative/NF-positive) that are immunoreactive for NF and MBP, but not for CGRP, NPY, and TH.
4. Noradrenergic sympathetic fibers (NPY-positive) that are immunoreactive for NPY and TH but not for CGRP, NF, and MBP.

Table 1 Clinical and AVS data from FM patients and control subjects

Age (Years)	FM Intensity Score	Visual Analog Scale (mm)	AVS Innervation area (mm^2) per Tunica Media Profile	Total Innervation Area (mm^2) of Largest AVS	CGRP/PGP Ratio	NF/PGP Ratio	NPY/CGRP Ratio
Fibromyalgia patients							
24	8.4	77	15	144	0.55	0.64	0.87
25	7.2	44	24	103	0.54	0.93	1.36
35	5.2	66	30	90	0.91	0.69	0.71
36	9.4	73	15	58	0.70	0.73	0.84
43	6.0	50	12	29	0.47	0.84	0.86
45	5.0	83	14	51	0.40	0.72	0.74
47	4.7	27	16	129	0.62	0.60	0.62
48	7.9	68	25	259	0.70	0.73	0.80
49	5.3	60	N/A	N/A	N/A	N/A	N/A
49	2.5	57	22	62	0.46	0.96	1.08
52	7.2	42	N/A	N/A	N/A	N/A	N/A
52	5.4	70	N/A	N/A	N/A	N/A	N/A
52	6.0	59	16	16	0.45	0.55	0.63
53	7.0	47	9	82	0.69	0.51	0.62
54	4.0	59	36	86	0.53	0.66	1.09
55	6.0	68	N/A	N/A	N/A	N/A	N/A
57	2.9	25	22	28	0.36	0.50	1.15
58	7.3	66	23	59	0.55	0.72	0.74
59	4.3	55	21	130	0.53	0.92	0.93
59	7.7	82	20	54	N/D	0.62	1.15
64	8.0	52	22	129	0.51	0.74	0.74
64	3.0	49	N/A	N/A	N/A	N/A	N/A
67	7.9	100	N/A	N/A	N/A	N/A	N/A
70	9.0	75	20	65	0.53	0.68	0.86
AVG 51	6.1	61	20	87	0.56	0.71	0.88
SEM 3	0.4	4	2	14	0.03	0.03	0.05
Control subjects							
22	N/A	N/A	N/A	N/A	N/A	N/A	N/A
24	N/A	N/A	10	10	N/D	0.57	N/D
25	N/A	N/A	N/A	N/A	N/A	N/A	N/A
29	N/A	N/A	N/A	N/A	N/A	N/A	N/A
33	N/A	N/A	N/A	N/A	N/A	N/A	N/A
35	N/A	N/A	4	35	0.46	N/D	0.76
39	N/A	N/A	17	17	0.36	0.75	N/D
39	N/A	N/A	N/A	N/A	N/A	N/A	N/A
39	N/A	N/A	12	17	0.4	0.62	1.68
40	N/A	N/A	9	41	0.25	0.74	1.32
40	N/A	N/A	N/A	N/A	N/A	N/A	N/A
42	N/A	N/A	7	9	0.42	0.54	1.06
45	N/A	N/A	5	7	0.52	0.79	0.85
47	N/A	N/A	6	21	0.36	0.69	1.57
51	N/A	N/A	N/A	N/A	N/A	N/A	N/A
54	N/A	N/A	N/A	N/A	N/A	N/A	N/A
56	N/A	N/A	19	30	0.39	0.92	1.78
59	N/A	N/A	N/A	N/A	N/A	N/A	N/A
63	N/A	N/A	22	36	0.33	0.77	1.20
64	N/A	N/A	5	14	N/D	N/D	2.44
65	N/A	N/A	7	17	0.29	0.65	1.48
65	N/A	N/A	7	27	0.36	0.42	2.04
74	N/A	N/A	10	25	0.22	0.86	1.45
AVE 47			10	22	0.36	0.69	1.47
SEM 3			2	3	0.04	0.07	0.22
T-test (FM vs CTL)							
P = 0.30			0.0001	0.0002	0.0001	0.77	0.0001

Participants were enrolled according to the study design and grouped accordingly into a fibromyalgia (FM) patient cohort and a control subject cohort. There were 24 FM patients and 23 control subjects examined for each group in total, and the average age among the study cohorts were not different. Among the FM patients, the fibromyalgia intensity score and the visual analog scale pain scores were remarkably consistent overall. AVS structures were identified in 18/24 FM and 14/23 control biopsies (average ages 49 and 48 years, respectively), and the innervation areas (mm^2) were determined. Innervation subset ratios (CGRP/PGP, NF/PGP, NPY/CGRP) were calculated using size (NF), sensory (CGRP), or sympathetic (NPY) neuropeptide immunodetectable expression levels.

AVS = arteriole–venule shunts; CGRP = calcitonin gene-related peptide; CTL = control; FM = fibromyalgia; N/A = no AVS in biopsy; N/D = no data; NPY = neuropeptide Y; PGP = protein gene product.

Therefore, immunofluorescence in this study was assessed using combinations of rabbit antihuman PGP9.5 (1:800; UltraClone LTD, Isle of Wight, UK), rabbit anti-CGRP (1:800; Millipore, Billerica, MA, USA), sheep anti-CGRP (1:800, AbCam, Cambridge, UK), mouse anti-200 kD NF protein (1:800, Sigma, St. Louis, MO, USA), sheep anti-NPY (1:800, Millipore). Based on preliminary assessments that CGRP-positive innervation expresses immunoreactivity for α2C receptors, a rabbit anti-α2C (1:400, Neuromics, Minneapolis, MN, USA) was also used. A separate slide of sections from each biopsy was processed for immunolabeling for each of the following: anti-PGP alone, CGRP/PGP, NF/PGP, CGRP/NF, NPY/CGRP, α2C/CGRP, and α2C/NPY. Double label combinations used the appropriate species of secondary antibodies conjugated with either Cy3 or Alexa488 (Jackson ImmunoResearch, West Grove, PA, USA; Molecular Probes, Eugene, OR, USA). Slides were preincubated in 1% bovine serum albumin and 0.3% Triton X-100 in PBS (PBS-TB) for 30 minutes and then incubated with primary antibodies diluted in PBS-TB overnight in a humid atmosphere at 4°C. Slides were then rinsed in excess PBS for 30 minutes and incubated for 2 hours at room temperature with the appropriate secondary antibodies diluted in PBS-TB. Following secondary antibody incubation, the sections were rinsed for 30 minutes in PBS and coverslipped under 90% glycerol in PBS. A number of unprocessed slides were archived under glycerol for future retrospective analyses with additional biomarkers.

Image Capture

Images were captured utilizing an Olympus DSU spinning disk confocal BX51-WI base microscope equipped with a Hamamatsu ER (Olympus America, Center Valley, PA, USA), DVC high-speed and Optronics Microfire cameras (Optronics, Goleta, CA, USA), 10 position LEP motorized filter wheel (Ludl Electronic Products Inc., Hawthorne, NY, USA), 3 axis motorized stage system, linear focus encoder, and Vistek vibration isolation platform (Vistek Inc, Tempe, AZ, USA), or an Olympus Optical Provis AX70 microscope (Olympus America) equipped with a high-resolution three-color camera (DKC-ST5; Sony, Montvale, NJ, USA). Both systems are equipped with conventional fluorescence filters (Cy3: 528–553 nm excitation, 590–650 nm emission; Cy2/Alexa 488: 460–500 nm excitation, 510–560 nm emission) and are linked to computers interfaced with NeuroLucida (MBF Bioscience, Essex, VT, USA) quantitative microscopy software, and Photoshop (Adobe Systems, San Jose, CA, USA) or Northern Eclipse (Empix Imaging, Mississauga, ON, Canada) image capture and processing software. For each IL, camera settings were kept the same for all image captures across all biopsies. Immunolabeling and innervation were quantified for AVS, arterioles, venules, and epidermal nerve fiber counts using NeuroLucida and Photoshop software. Quantitative results were compared between the FM patients and the healthy control subjects by Student's *t*-test or Wilcoxon Rank Sum test, with significance set at $P < 0.05$.

Quantification of Arteriole and AVS Innervation

Quantification of the dense, compact innervation of arterioles and AVS consisted of: 1) the area occupied by the innervation located around the perimeter of each arteriole and AVS profile within each section, and 2) the relative proportions of different types of innervation affiliated with each profile. To determine the area of innervation, each arteriole or AVS profile was located in a slide of sections processed only for PGP immunofluorescence for each biopsy. NeuroLucida routines were used to trace the contour and calculate the enclosed area of the vessel lumen, the smooth muscle vessel wall (tunica media), and the immunolabeled innervation in the surrounding tunica adventitia.

To determine the relative proportions of different types of arteriole and AVS innervation, different slides of sections from each biopsy were used that were double labeled using different pairs of primary antibodies detected with appropriate species of Cy3 (red) or Alexa 488 (green) conjugated secondary antibodies. The relative proportions for the following double label combinations were quantified:

1. CGRP (Cy3) and PGP (Alexa 488) to determine what proportion of the total innervation (green channel) was uniquely CGRP (red channel) containing sensory innervation.
2. NF (Cy3) and PGP (Alexa 488) to determine what proportion of the total innervation (green channel) was Aδ-fiber (red channel) sensory innervation.
3. NPY (Cy3) and CGRP (Alexa 488) to determine what proportion of the innervation was NA sympathetic (red channel) and CGRP sensory (green channel).

Because inter-subject quantification of IL intensity is limited by several variables (i.e., individual antibody mixes for each processing day and different biopsies), the relative proportions of label luminescence was assessed for each arteriole and AVS profile in every section on each slide for each biopsy. The areas occupied by the innervation for each arteriole and AVS profile were circumscribed using Photoshop tools and the average luminescence of the circumscribed area was determined for the red and green channels. The average luminescence values for the red and green channels within the circumscribed area were then utilized to create relative proportion for each double label combination. Resulting proportions were subsequently averaged from all the double-labeled arterioles and AVS profiles in each biopsy. As the luminescence is a function of both the density and intensity of each labeled pixel, this approach provides a relative comparison between the proportions of different arteriole and AVS innervation types within control subject and FM patient biopsies.

Quantification of Venule Innervation

Unlike arterioles and AVS, cutaneous venules have sparse innervation. This innervation was quantified by

using NeuroLucida routines to trace the outer contour of the venous wall and then to map the location of nerve fiber along the contour. Innervation density was expressed as the number of profiles per unit length of each outer venule contour.

Epidermal Innervation

The epidermal innervation density was quantified in the hypothenar and thoracic biopsies of the nine control subjects and nine age-matched FM patients. Using NeuroLucida software, complete montages of three PGP9.5 immunolabeled sections taken at approximately one-third intervals through each biopsy were captured, and the total number of intraepidermal nerve fiber profiles that were observed to be in contact with the basement membrane were determined. The values were subsequently divided by the length of the epidermis to determine the intraepidermal nerve fiber densities (IEFD) for each biopsy.

Results

Clinical

The FM subjects ranged in age from 24 to 74 (average age 47 years) and the control subjects ranged from 22 to 70 years old (average age 51 years), and was not significantly different (Table 1, $P = 0.30$). The average ages of the 18 FM patients and 14 control subjects utilized for AVS analysis were 49 and 48 years, respectively. At initial screening visits, the patient average FM intensity score (FIS) and VAS were 6.0 ± 2.0 and 60.0 ± 18.0, respectively. This is consistent with moderate to severe pain. Control subjects reported no pain; FIS and VAS were not recorded.

Vascular Morphology

Hypothenar Biopsies

As seen in sections from hypothenar skin biopsies, profiles of arterioles, venules, and AVS have various morphologies depending upon how they are cut by the plane of sectioning (Figures 1 and 2). Arterioles ramify throughout the deep dermis and appear in at least some sections of all biopsies as individual profiles with mostly uniform circular to oval shapes of varying lengths (solid arrows in Figures 1 and 2). Arterioles often have an open lumen surrounded by a uniformly thick smooth muscle tunica media, enveloped by a tunica adventitia composed of collagen bundles, and which contains dense innervation of both sympathetic and sensory origin [19,45]. Venules typically have irregular contours with a relatively thin tunica media, an open irregular lumen, and very sparse innervation discontinuously spaced around the perimeter of the tunica media (open arrows in Figure 1). Arteriole and venule profiles were encountered in the hypothenar biopsies from 21 of the 23 control subject biopsies and from 21 of the 24 FM patient biopsies.

AVS occur at discreet locations within the vascular tree as short, tortuous, direct connections between an arteriole and a venule, where they function as valves to shunt blood flow either into or to bypass terminal capillary networks for thermoregulatory mechanisms. Due to their tortuous shape, a section passing through an AVS

Figure 1 Images of arteriole–venule shunts (AVS) profiles labeled with anti-protein gene product (PGP) in sections of hypothenar skin biopsies from control subjects (A, C, E, G, I) and from comparable age fibromyalgia (FM) patients (B, D, F, H, J). The images represent the largest shunt profiles encountered among the sections from each biopsy. Due to the tortuous nature of the AVS structures, the plane of section through an AVS creates multiple profiles of varied shapes (asterisks) which reveal a constricted lumen and thick tunica media. Tunica media profiles have similar areas in the control and FM biopsies specimens, indicating that the AVS smooth muscle has not enlarged. AVS connect to an entering arteriole at one end (solid arrows) and an exiting venule at the other end (open arrows). The arterioles have a well-developed, albeit thinner, tunica media than the AVS and are not tortuous resulting in single, uniformly round to oval profile with an open lumen. They are surrounded by a uniformly dense perimeter of innervation. A plane of section containing the connection of the arteriole to the AVS can be seen in C and I. The profiles of the arterioles and their surrounding innervation are comparable in size in the control subject and FM patient biopsies. A relatively large arteriole located deeper in the dermis that does not directly supply an AVS is shown in H (large arrow). Venule profiles generally have a thinner tunica media and larger lumen than the arteriole profiles, resulting in an irregular shape, and are surrounded by sparse discontinuous innervation. Each individual profile in the AVS is surrounded by dense anti-PGP labeled innervation which is far greater in the FM patient biopsies compared with control subjects, resulting in a greatly enlarged AVS size. Each Scale bar = 50 μm.

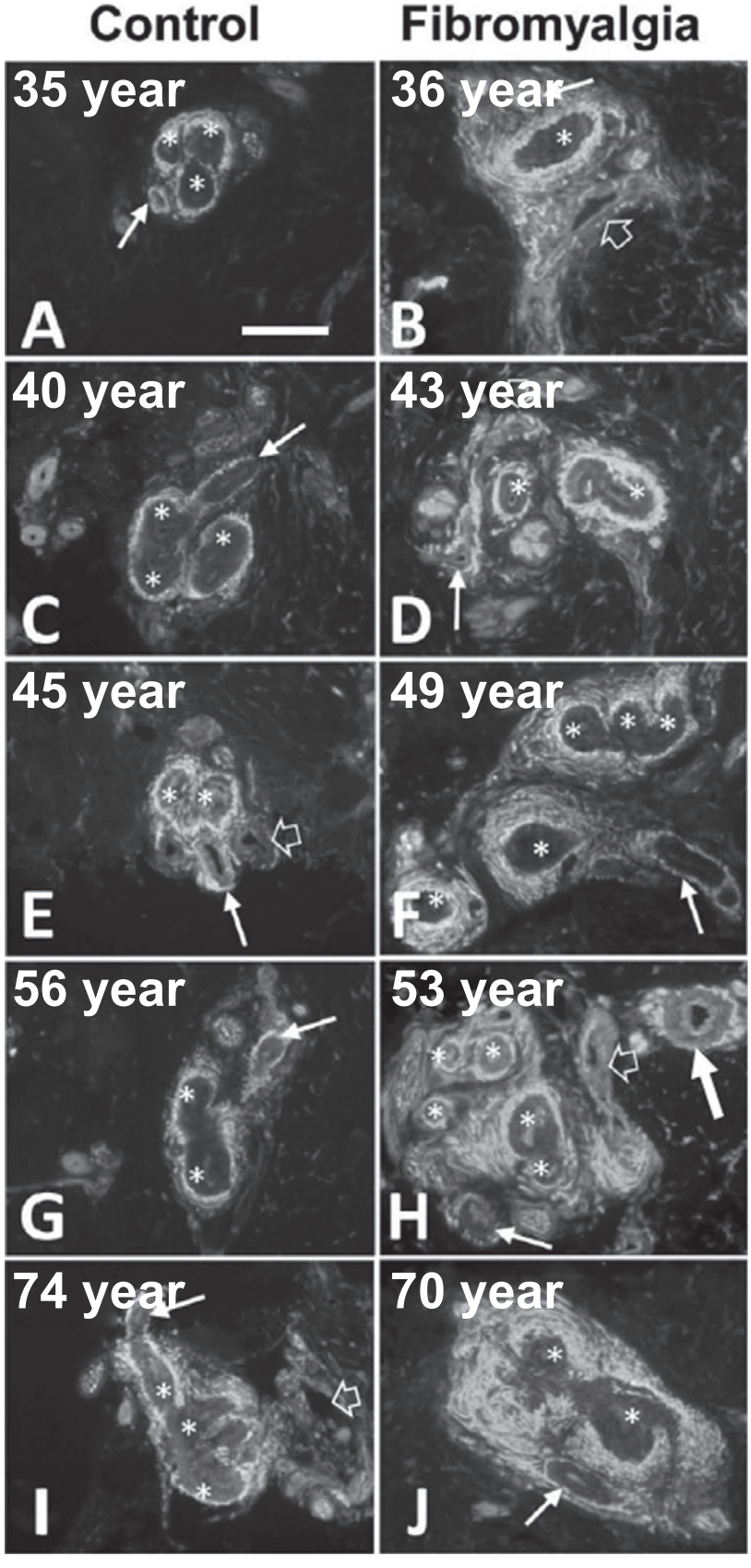
Control
Fibromyalgia
35 year
A
36 year
B
40 year
C
43 year
D
45 year
E
49 year
F
56 year
G
53 year
H
74 year
I
70 year
J

can result in several circular, oval, or s-shaped vessel profiles (asterisks in Figures 1 and 2). The tunica media of each AVS profile is much thicker than that of an arteriole profile, the lumen is typically more constricted, and the tunica adventitia is thicker and more densely packed with innervation. AVS profiles were obtained in the hypothenar biopsies from 14 of the 23 control subjects and 18 of the 24 FM patients. In certain planes of sectioning, an arteriole can be seen entering and connecting to the AVS (Figures 1A,I) and a venule can be seen leaving the AVS (Figure 1H).

Thoracic Biopsies

The deep dermis of thoracic biopsies had few vascular profiles, and those present were far smaller than those in the hypothenar biopsies. Presumptive arterioles had a thin perimeter of innervation and presumptive venules had little if any innervation. There were no AVS profiles.

Vascular Innervation

Anti-PGP9.5 labels for an enzyme highly enriched in neuroedocrine cells which is normally expressed in all known peripheral innervation. PGP9.5 immunolabeling reveals the totality of the vascular innervation (Figure 1), which can be subtyped through immunolabeling for other specific antigens. Normal sympathetic innervation of cutaneous arterioles consists of unmyelinated noradrenergic fibers that have been previously shown to express TH and to IL for anti-NPY. The NPY-positive sympathetic innervation is concentrated at the perimeter of the tunica media (Figure 2G). Normal sensory innervation of arterioles is more diffusely distributed in the tunica adventitia and consists predominately of presumptive C fibers that label with anti-CGRP, but not with anti-NF (Figure 2A,E,G). A smaller contingent of sensory innervation consists of presumptive Aδ fibers that label with anti-NF, and which have previously been shown to IL for anti-MBP (Figure 2C). A minority of

Figure 2 Images of serially sectioned arteriole–venule shunts (AVS) from a control subject and an age-matched fibromyalgia (FM) patient showing immunoreactive labeling (IR) of alternating sections with different antibody combinations which reveal different subtypes of vascular innervation. Panels of three images show the merged double labeling (top image) with antibodies against the antigens indicated as revealed by red and green fluorophore-tagged secondary antibodies. The separate channel individual antigen labeling is shown at half magnification (lower images). Colocalization of the two antigens appears yellow in the merged images. Asterisks indicate the AVS profiles within the sections, and arrows indicate the arterioles that are connected to the AVS. (A,B) calcitonin gene-related peptide-immunoreactive labeling (CGRP-IR) (red) reveals nearly all of the C fiber and a subset of Aδ fiber sensory innervation, whereas protein gene product-immunoreactive labeling (PGP-IR) (green) reveals all types of sensory and sympathetic innervation. Therefore, innervation expressing CGRP-IR appears yellow in the merged image, and that which lacks CGRP-IR appears green. The innervation that is only green includes mostly Aδ types of sensory fibers and the sympathetic fibers. In the FM patient (B), the vast increase in the AVS innervation involves the CGRP-IR innervation. (C,D) neurofilament- immunoreactive labeling (NF-IR) (red) reveals all of the likely Aδ sensory fiber innervation, whereas PGP-IR (green) reveals all innervation. Therefore, the Aδ fibers are yellow in the merged image, whereas the C-fiber sensory innervation and the sympathetic innervation appear only green. The NF-IR innervation is also increased in the FM patient AVS (D). (E,F) CGRP-IR labeling alone is limited to small-caliber C-fiber sensory innervation (red) and NF-IR labeling alone (green) is limited to all Aδ fiber nonpeptidergic sensory innervation. Yellow labeling reveals CGRP containing Aδ fibers. All of this innervation is increased in the FM patient AVS profiles. (G,H) NPY-IR (red) reveals a densely packed small-caliber sympathetic innervation, while CGRP-IR (green) is localized to C-fiber sensory innervation. Both types are closely intermingled and intertwining, resulting in a yellow appearance. Although both types of innervation are increased in the FM patient AVS, quantification of these two sets of innervation reveals that the CGRP innervation is increased proportionately more than the neuropeptide Y (NPY) innervation (see Figure 3I). (I,J) α2C-IR (red) is expressed mostly, if not entirely, on CGRP-containing C fibers that are closely intermingled with the NA/NPY-expressing sympathetic innervation. Both are increased in the FM patient AVS profiles, indicating that the increased sensory innervation within the FM patient AVS likely retains NA responsiveness. Scale bar = 50 μm.

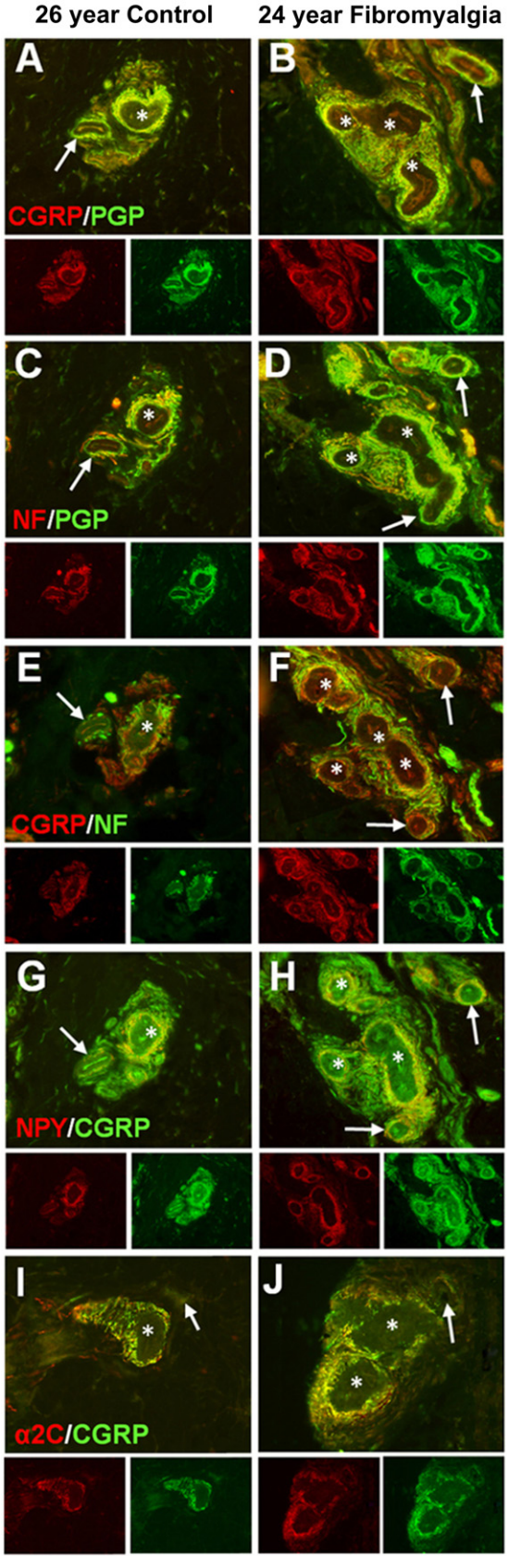
26 year Control
24 year Fibromyalgia
A
B
CGRP/PGP
C
D
NF/PGP
E
F
CGRP/NF
G
H
NPY/CGRP
I
J
α2C/CGRP

the Aδ innervation colabels with anti-CGRP (Figure 2). The control AVS profiles were innervated by a similar mix of sympathetic and sensory axons, but which was at least 2× greater in quantity compared with an innervated arteriole. Importantly, double labeling with anti-α2C (NA receptor) and anti-CGRP (Figure 2I,J) demonstrated that α2C was largely coexpressed on CGRP positive C fibers. Double labeling for anti-α2C and anti-NPY revealed that the α2C-expressing peptidergic sensory C fibers are closely intermingled with the NPY-expressing sympathetic innervation.

Increased Size of AVS in FM

AVS profiles from FM patients were dramatically larger in size compared with those in age-matched control subjects (Figure 1). As a reflection of their larger size, AVS were present in the hypothenar palm biopsies of 18 out of 24 FM patient biopsies (75%) compared with 14 out of 23 control subject biopsies (61%), and AVS profiles were encountered ~3× more frequently among the individual biopsy sections from FM patients compared with control subjects. The total average area occupied by complete AVS profiles among FM patients was significantly increased compared with control subjects (Figure 3A, $P < 0.001$). Importantly, serial reconstructions revealed that there were *not* increased numbers of AVS per biopsy in FM patients compared with control subjects (Figure 3B, $P = 0.11$), indicating that the AVS had increased in size.

To assess what components were contributing to the increased size of the FM AVS, NeuroLucida mapping routines were applied to PGP9.5 labeled sections from every FM patient and control subject biopsy that contained an AVS. Profiles were mapped to determine: 1) the area of the tunica media of each AVS profile (Figure 3C); 2) the number of tunica media profiles (with lumen) per AVS (Figure 3D); and 3) the area containing the innervation affiliated with each AVS profile (Figure 3E,F). These metrics were also determined for the arteriole profiles within sections from each hypothenar biopsy that contained arteriole profiles (Figure 4A–C).

Tunica Media

No significant difference was detected in the average cross-sectional areas of the tunica media profiles encountered among the AVS from control subject compared with FM patient biopsies (Figure 3C, $P = 0.83$), indicating that

Figure 3 Quantification and statistical comparisons of arteriole–venule shunts (AVS) innervation parameters in the hypothenar palm skin of fibromyalgia (FM) patient and control subject biopsies. White bars are control subjects, black bars are FM patients. (A) Increased AVS size was observed as a significantly greater total area (mm^2) of innervation within sections from FM patient compared with control subject biopsies. (B) Serial reconstruction revealed that the average number of AVS per biopsy was not significantly higher in FM patient compared with control subject biopsies, including biopsies absent of detectable AVS (N = 24 and N = 23, respectively). (C) Single AVS structures have a tortuous shape and are typically cut several times by the plane of sectioning, resulting in several lumen and tunica media (smooth muscle) surrounds in each AVS profile. The cross-sectional area of the tunica media profiles within each AVS was virtually identical in the FM patient compared with control subject biopsies, indicating that the size of the vessel musculature was not significantly different. (D) Examining the number of tunica media occurrences within each AVS profile revealed a significant increase among the FM patient compared with control subject biopsies, indicating an increased degree of AVS tortuosity. (E) AVS innervation area per tunica media occurrence demonstrated significantly increased innervation among the FM AVS compared with control AVS. F. Measuring the single largest complete AVS profile encountered among the sections within each biopsy also revealed a highly significant increase in the total innervation in the FM patient compared with control subject biopsies. (G–I) Multimolecular immunolabeling proportions were performed on a subset of FM and control biopsies, excluding two controls and one FM where values were missing (see Table 1, N/D). (G) The calcitonin gene-related peptide (CGRP) to protein gene product (PGP) innervation ratio was significantly greater among AVS structures in FM patient compared with control subject biopsies. (H) The neurofilament (NF) to PGP innervation ratio remained virtually identical between the groups. (I) The neuropeptide Y (NPY) to CGRP innervation ratio was significantly lower in FM patient compared with control subject biopsies. Taken together, these results indicate a significantly increased sensory and/or decreased sympathetic innervation among AVS in FM patients compared with age-matched control subjects.

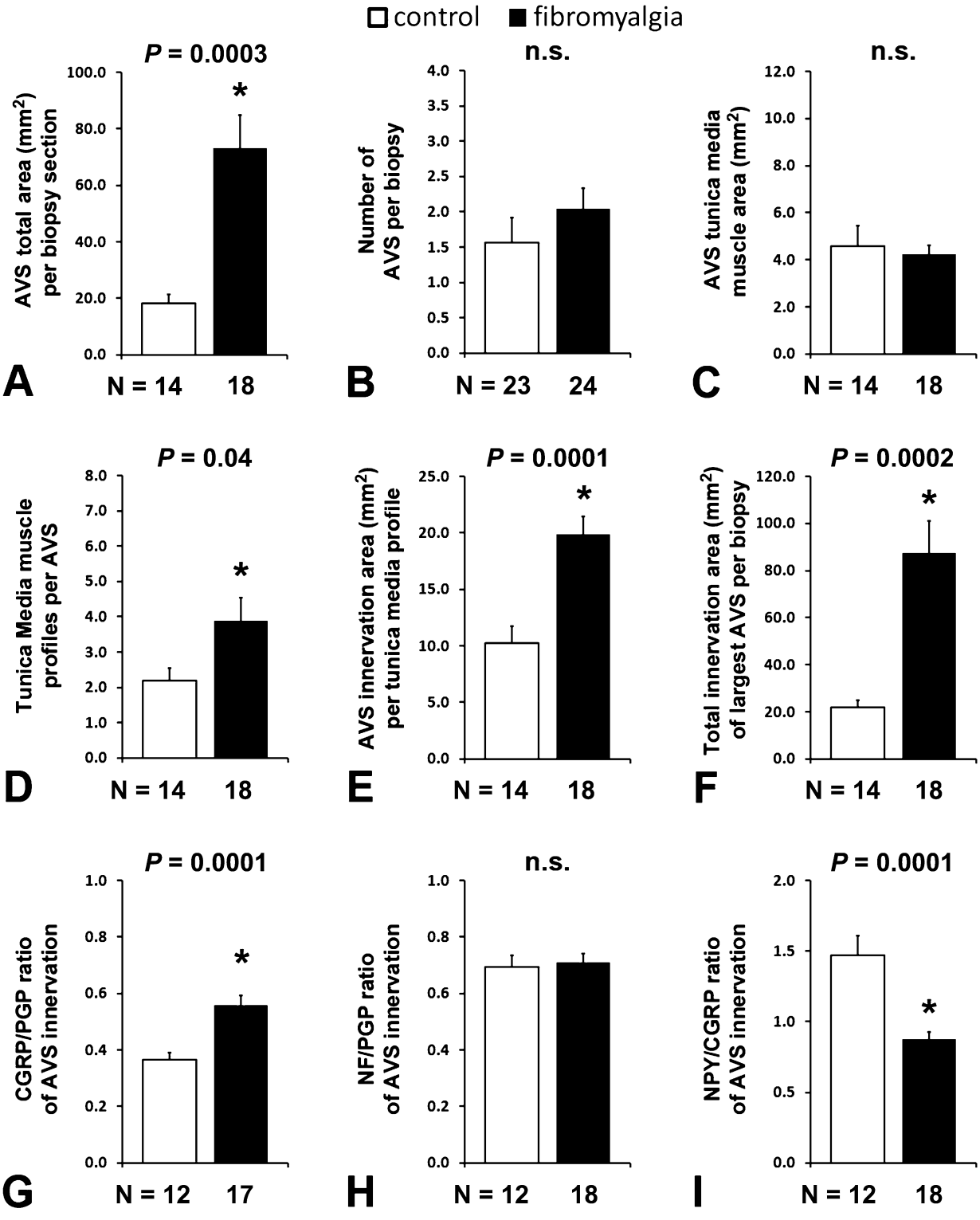
control
fibromyalgia
P = 0.0003
AVS total area (mm2) per biopsy section
100.0
80.0
60.0
40.0
20.0
0.0
*
A
N = 14
18
n.s.
Number of AVS per biopsy
4.0
3.5
3.0
2.5
2.0
1.5
1.0
0.5
0.0
B
N = 23
24
n.s.
AVS tunica media muscle area (mm2)
12.0
10.0
8.0
6.0
4.0
2.0
0.0
C
N = 14
18
P = 0.04
Tunica Media muscle profiles per AVS
8.0
7.0
6.0
5.0
4.0
3.0
2.0
1.0
0.0
*
D
N = 14
18
P = 0.0001
AVS innervation area (mm2) per tunica media profile
25.0
20.0
15.0
10.0
5.0
0.0
*
E
N = 14
18
P = 0.0002
Total innervation area (mm2) of largest AVS per biopsy
120.0
100.0
80.0
60.0
40.0
20.0
0.0
*
F
N = 14
18
P = 0.0001
CGRP/PGP ratio of AVS innervation
1.0
0.8
0.6
0.4
0.2
0.0
*
G
N = 12
17
n.s.
NF/PGP ratio of AVS innervation
1.0
0.8
0.6
0.4
0.2
0.0
H
N = 12
18
P = 0.0001
NPY/CGRP ratio of AVS innervation
2.0
1.5
1.0
0.5
0.0
*
I
N = 12
18

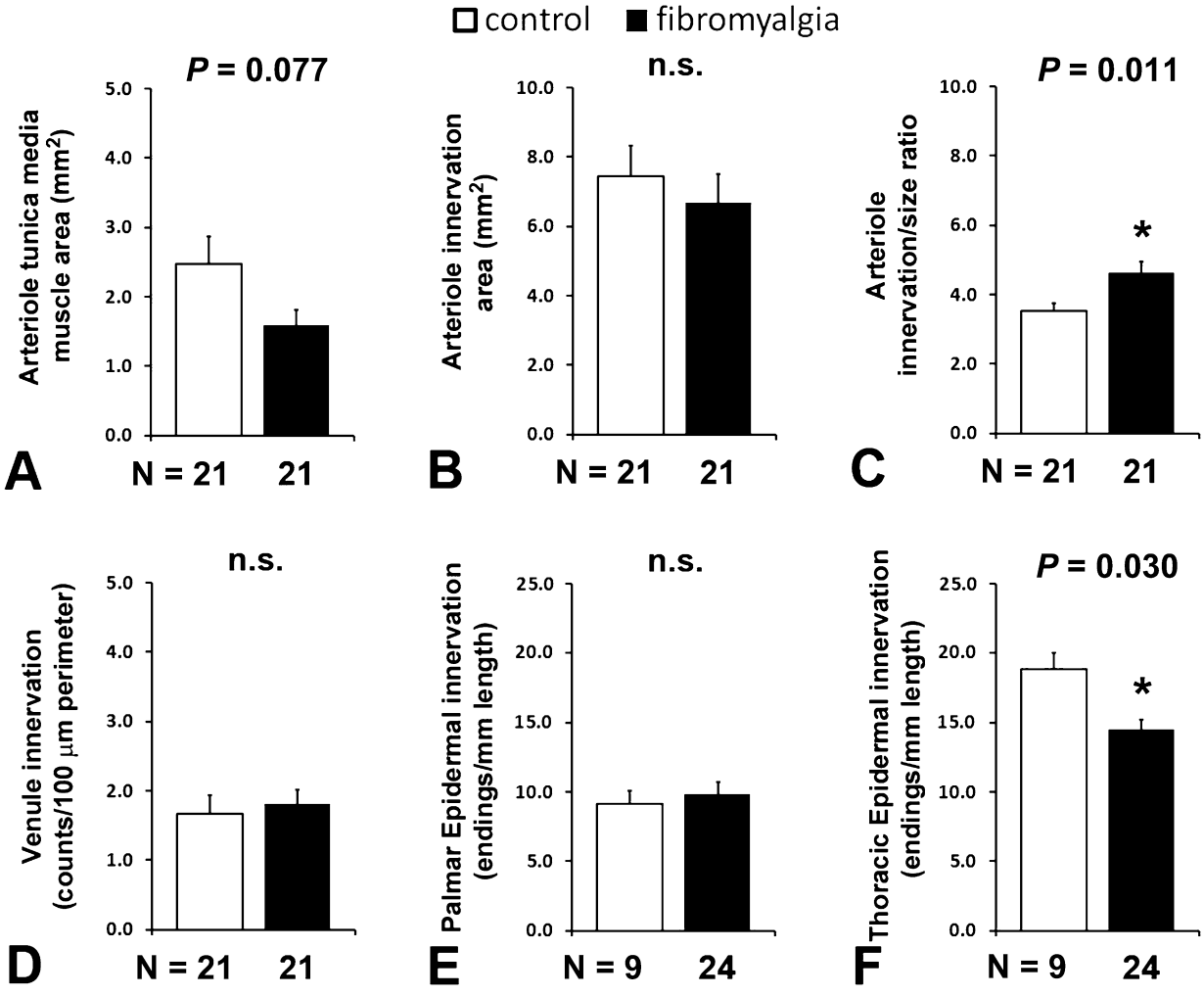

Figure 4 Quantification and statistical analysis of arteriole parameters (A,B,C), venule parameters (D), and epidermal innervation density (E,F). (A) The average cross-sectional tunica media (smooth muscle) areas of the arteriole profiles in control subject compared with fibromyalgia (FM) patient biopsies was not significantly different, but did trend toward smaller sized FM vessels ($P = 0.077$). (B) The average innervation area surrounding the arteriole profiles was not significantly different between the groups. (C) Normalizing the arteriole innervation area by tunica media size uncovered a significant increase in innervation among the FM patient compared with the control subject biopsies. (D) The average density of innervation around the perimeter of venule profiles was not significantly different between the groups. (E,F) The average intraepidermal nerve fiber densities (IEFD) of immunolabeled profiles crossing the basement was not significantly different in the palmar skin (E), however was significantly reduced (78%, $P = 0.030$) among the back skin biopsies of FM patients compared with control subjects (F).

the smooth muscle had not hypertrophied in the FM patients. Similarly, no significant difference was found among the cross-sectional areas of arterioles from control subject compared with FM patient biopsies (Figure 4A). To determine whether the AVS had became more tortuous, the number of tunica media profiles associated with each sectioned AVS was assessed. FM patient AVS did show a slight but significant increase in tortuosity compared with control biopsies (Figure 3D, $P = 0.04$).

AVS Innervation

Quantification of the area occupied by the innervation to each AVS revealed a highly significant increase among FM

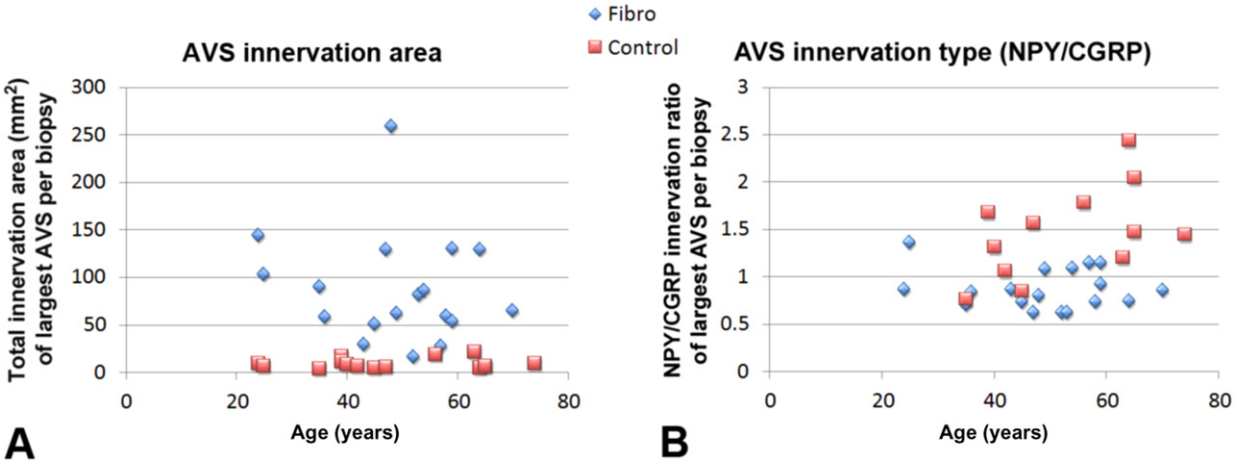

Figure 5 Scatter plot analysis of arteriole–venule shunts (AVS) innervation area and type. (A) Innervation area analysis of the largest AVS profiles from fibromyalgia (FM) patient and age-matched control biopsies demonstrates a significant increase in AVS profile size associated with FM diagnosis. The data spread across ages further indicate the very limited total overlap among the groups, where only a single FM profile appeared smaller than the three largest control profiles, and only a single control biopsy was larger than the three smallest FM profiles. Also note that at each specific age, the FM profiles were always larger compared with control subjects. (B) The neuropeptide Y/calcitonin gene-related peptide-immunoreactive labeling (NPY/CGRP-IR) ratios measure the relative proportions of vasoconstrictive sympathetic to vasodilatory sensory innervation. Control AVS innervation generally contains more sympathetic (NA/NPY-expressing) compared with sensory (CGRP-expressing) innervation (e.g., ratios greater than 1) which increases across age. FM ratios are significantly skewed to increased sensory innervation, and remain increased across ages. Also note that at each specific age, the FM ratios were always skewed to increased sensory innervation compared with control subjects.

patients compared with control subjects. The results demonstrate that the *overall average* innervation area of AVS profiles were two times greater in FM patient than control subject biopsies (Figure 3E: 20×10^3 μm [2] vs 10×10^3 μm [2], respectively, $P < 0.001$). Furthermore, the total area occupied by innervation from the *single largest* AVS profile identified from each biopsy demonstrated an innervation area that was four times greater in the FM patient compared with control subject biopsies (Figure 3F: 87×10^3 μm [2] vs 22×10^3 μm [2], respectively, $P < 0.001$). There were no significant differences in the innervation area surrounding the arterioles (Figure 4B); however, when arteriole innervation area was normalized by tunica media size, a slight but significant increase in arteriole innervation among the FM patient biopsies was detected (Figure 4C, $P = 0.011$). There were no significant differences in the innervation area surrounding venules (Figure 4D) from FM patient compared with control subject biopsies.

Additionally, there was only very limited overlap between the ranges of AVS innervation areas from FM patient compared with control subject biopsies, regardless of age (Figure 5A). Furthermore, the innervation area remained similar across age in the control subjects, whereas the exuberant innervation areas varied dramatically across the FM patient cohort. Importantly, at every age-matched comparison, the AVS innervation areas from FM patient biopsies were always significantly greater than control biopsies (Figure 5A).

Altered Proportions of Sensory/Sympathetic AVS Innervation

Initial qualitative assessments of double label combinations indicated that peptidergic (CGRP-containing) sensory axons disproportionately contributed to the increased AVS innervation (Figure 2A,B). Therefore, a quantitative assessment was also conducted to determine whether the increased AVS innervation observed in FM patients involved a differential shift in the functional type of axons, as assessed by IL combinations for CGRP, NF, NPY, and PGP. These quantitative analyses were conducted on all biopsies that contained AVS profiles. The results demonstrate that the CGRP-positive innervation was disproportionately represented in FM patient AVS profiles compared with control subject AVS profiles (Figure 3G, $P < 0.0001$). By contrast, the average

proportion of NF-IL to PGP-IL luminescence (Figure 2C,D) was virtually identical between the FM patient and control subject AVS profiles (Figure 3H, $P = 1.04$). Results from CGRP-IL and NF-IL revealed that only a small proportion of the total Aδ fiber innervation among AVS profiles was peptidergic (CGRP positive) from either the control subject or FM patient biopsies (Figure 2E,F). Furthermore, a comparison of NPY-IL and CGRP-IL combinations (Figure 2G,H) revealed that the proportion of NPY-expressing sympathetic innervation was significantly decreased relative to the CGRP expressing sensory innervation in the FM patient AVS profiles (Figure 3I, $P < 0.0001$). Taken altogether, these results demonstrate that the sensory peptidergic C-fiber innervation has increased to a greater degree than the Aδ fiber innervation, and has resulted in a significantly increased ratio of CGRP-expressing vasodilatory sensory innervation to noradrenergic vasoconstrictive sympathetic innervation among the FM patient AVS profiles compared with control subjects (Figure 5B).

Thoracic Skin Biopsies

A routine subjective assessment of arterioles and venules among the thoracic skin biopsies from FM patients and control subjects did not reveal any potential differences between the vascular profiles or innervation.

Epidermal Innervation

Epidermal innervation density was assessed in the hypothenar and thoracic biopsies from the nine control subjects specifically recruited for this study, and in nine age-matched FM patients. No differences were detected between the IEFD among hypothenar palmar control subject and FM patient biopsies (Figure 4E). In contrast, the thoracic back skin of FM patients did show a significant (~20%) decrease in IEFD compared with control subjects (Figure 4F, $P = 0.03$), consistent with observations of decreased IEFD in other chronic pain skin conditions, and recently also demonstrated in FM [18,63–64]. Interestingly, based upon the counting procedures utilized, the overall IEFD counts were lower in the palmar skin compared with the thoracic skin. Total counts of epidermal endings, which included PGP-positive ending profiles not found to be in contact with the basement membrane, also did not reveal any difference between FM patient and control subjects for the thoracic back skin or hypothenar palmar skin (data not shown).

Discussion

A major finding in this study revealed that the AVS in palmar glabrous skin biopsies of FM patients had excessive sympathetic and sensory innervation compared with normal control subjects, whereas innervation to arterioles and venules appeared normal. The CGRP-positive vasodilatory sensory innervation appeared significantly increased compared with the NYP-positive vasoconstrictive sympathetic innervation among the AVS. AVS have an especially thick tunica media and form short, valve-like connections directly between arterioles and venules, where they presumably function in concert with resistance arterioles to provide dynamic control of blood flow to the superficial capillaries [19,43,45,47,65–66]. In human and nonhuman primates, the glabrous skin of the hands and feet has a particularly high surface to volume ratio with a high capillary density and plays a major role in thermoregulation and the maintenance of core body temperature as well as the apportionment of blood to other organs such as skeletal muscle during periods of high metabolic demand. Therefore, the particularly excessive sensory innervation of the AVS in the palmar skin of FM patients may contribute to extreme tenderness and pain in the hands, but may also contribute to the chronic widespread deep pain, fatigue, sleep disturbances, and cognitive dysfunction associated with FM.

Chronic pain research is focused primarily on two well-defined mechanisms which are not mutually exclusive. The first involves aberrant hypersensitivity and hyperactivity of the primary sensory neurons (nociceptors) in the PNS that are the inputs to central pain pathways, i.e., “irritable nociceptors,” while the second involves hyperresponsivity of pain pathway CNS neurons, particularly dorsal horn or thalamus, i.e., “central sensitization” [19,45]. Hypersensitivity and hyperactivity of primary sensory neurons has particularly been implicated in chronic pain associated with such neuropathic conditions as postherpetic neuralgia (PHN), complex regional pain syndrome (CRPS), painful diabetic neuropathy, and erythromelalgia, where pathologies have been documented among the small-caliber innervation to the epidermis and upper dermis, and signaling mechanisms of keratinocytes [18–19,24,26,62,67]. The pain symptoms associated with these conditions typically include combinations of thermal, chemical, and/or mechanical hyperalgesia and allodynia, as well as spontaneous burning pain perceived as originating primarily from the skin surface and localized to a specific location of the body. By contrast, FM has been attributed primarily to a central sensitization disorder due to the widespread diffuse deep pain, lack of direct evidence of a PNS pathology, and the partial therapeutic benefit of SNRI and calcium channel modulators that are regarded as acting primarily in the CNS. The diffuse deep tissue pain is presumed to originate from sensitized CNS responsiveness to deep tissue afferents with some indications that such afferents may also be hyperactive due to an unknown source of deep tissue ischemia.

Our study examined the innervation in biopsies from two sites: 1) thoracic hairy skin overlying the trapezius area tender point used to diagnose FM; and 2) the hypothenar glabrous skin of the hand. The hands in FM patients are typically among the most painful locations, although they not included as specific diagnostic tender point likely because pain in the hands also occurs in a variety of other disorders [1,18,34–35,68–71]. As such, the hands have been used in many studies designed to assess altered tactile sensation and changes in various pain thresholds in FM patients [17,29,36,42,72–73]. In FM, a “first pain” mechanical pressure allodynia has been observed

followed by a delayed "second pain" heat hyperalgesia. The immediate pressure allodynia is attributed to hypersensitivity among unidentified cutaneous mechanoreceptors, whereas the delayed heat hyperalgesia is attributed to sensitization of neurons in the CNS [5–6,10,42,74–75]. However, the source and maintenance of the hypothesized central sensitization is unknown [4–5,10,76–77].

A reduction of small-caliber nociceptor epidermal innervation has been detected in a variety of chronic painful neuropathic conditions such as CRPS, diabetic neuropathy, and PHN [18,20–22,25,67,70,78–80]. The seeming paradox of chronic pain associated with reduced nociceptor (pain) innervation has been partially explained by physiological evidence of hypersensitivity among the remaining innervation, which could be exacerbated by increased purinergic signaling and CGRP upregulation among epidermal keratinocytes [24,26,45,81–82]. However, reduced epidermal innervation does not always manifest chronic pain, and chronic pain is not always accompanied by reduced epidermal innervation. Recently, a significant loss of epidermal fibers from nonglabrous forearm and leg skin of FM patients has now been reported [63]. Consistent with this observation, we detected 20% less nerve fibers entering the epidermis in the thoracic biopsies of FM patients compared with normal subject biopsies. We did not observe a difference among the epidermal innervation of hypothenar palmar skin biopsies. Although the loss of epidermal endings, accompanied by hyperexcitability of remaining endings might contribute to widespread pain, the decrease observed among the FM patients was not as severe as documented in other painful conditions, and furthermore, the loss of epidermal innervation is not intuitively consistent with the deep pain characteristic of FM patients.

We chose to biopsy the glabrous hypothenar skin to specifically investigate the innervation to arterioles and AVS as a potential site of FM related pathology in the PNS, particularly as these targets are located deep in the skin and are a major site of convergence for dense sympathetic and sensory innervation. The arterioles and AVS are innervated by dense NA sympathetic innervation, and also several molecularly distinct subtypes of small-caliber sensory innervation [19,43,46–47,62,83]. The vast majority is peptidergic C-fiber innervation containing CGRP and SP, while a smaller, albeit substantial, contingent of the sensory innervation is composed of Aδ fibers, of which subsets can express or lack CGRP and SP. More recently, it has been established that subsets among the C and Aδ fibers express various combinations of ligand-gated receptors and ion channels, such as TrpV1, TrpA1, ASIC3, and/or H3R, each of which are implicated in mechanoreceptive, metaboreceptive, thermoreceptive, and various nociceptive capabilities attributed to small fiber afferents [18,44,84–85].

To date, the function of the multiple varieties of arteriole and AVS sensory innervation has received little attention. The literature on the neural vasoregulation of the glabrous skin has focused almost entirely on sympathetically mediated vasoconstriction caused by NA and NPY activation of the smooth muscle tunica media [86–88]. The dilation of the arterioles and AVS is widely regarded as a passive consequence of reduced sympathetic activity or the dilatory action of compounds such as NO released from endothelial cells [89]; however, there is little mention of sensory feedback mechanisms operating among microvasculature to regulate blood flow. It is well established that CGRP and SP are potent vasodilators and that heat stimulation of peptidergic sensory endings in the skin can elicit a local "axon-reflex" effector release of CGRP and SP from collateral branches terminating among capillaries and precapillary arterioles [50,86,90–97]. Presumably, the extensive peptidergic sensory innervation to the arterioles and AVS serves an important vasodilatory role as well, particularly as the arteriole smooth muscle has also been shown to express appropriate peptidergic receptors [98]. We recently reported that cutaneous vascular sensory innervation may also contribute to a variety of conscious mechanical and thermal tactile sensations, as well as pain [43]. Aδ fibers innervating arterioles and AVS may particularly include low threshold mechanoreceptors whose primary role is to detect stretch and/or tension in the vessel walls in response to blood pressure [19].

Importantly, we found that the peptidergic sensory innervation to the arterioles and AVS coexpress α2C receptor immunoreactivity. Previous studies have shown that NA activation of an α2 receptor mechanism can inhibit the release of CGRP and SP [99]. Therefore, sympathetic release of NA may mediate vasoconstriction not only by direct constriction of the tunica media smooth muscle, but also by blocking the vasodilatory peptide release from vascular afferents [56,58,100–101].

Our multilabeling analyses revealed that nearly all of the AVS obtained in hypothenar biopsies from FM patients had excessive innervation. The excessive innervation included Aδ fibers (defined as NF-positive), but was significantly skewed toward an overrepresentation of CGRP-expressing innervation, which consists mostly of C fibers (defined as NF-negative, NPY-negative), and an underrepresentation of NA sympathetic innervation [19,43,47,83]. Furthermore, even though AVS branch directly from the arterioles, only a slight excess in arteriole innervation was detected among the FM patients, and there were no indications that the proportions of arteriole sensory or sympathetic innervation differed between FM patient and control subjects. Taken together, these data indicate that FM patients have a neurovascular pathology in the palms of the hands predominantly increasing the peptidergic sensory innervation of the AVS.

Although Aδ fibers are not disproportionately represented in the AVS of FM patients, they are excessive compared with those in the AVS of control subjects and, therefore, may contribute to the symptoms of fast pain pressure allodynia elicited from the palms of FM patients.

Furthermore, heat thermal functionality is presumably among the peptidergic C fibers which are known to express TrpV1, and prolonged exposure to capsaicin diminishes heat-induced vasodilatory and consequent inflammatory responses [18,44,88]. Thus, the increased peptidergic C-fiber innervation among the FM patient AVS could be a source of the observed heat hyperalgesia, although the relative delay and windup of the heat hyperalgesia has been interpreted as an indicator of central sensitization [10,16–17,39,74–76]. The central terminals of the excessive peptidergic innervation of the AVS may contribute to abnormally high levels of vasodilatory peptides previously documented in the CSF of FM patients [102].

Of particular note, relative to the excess sensory innervation of the AVS, is the extreme sensitivity of the FM patients to cold stimuli and the exacerbation of FM symptoms especially by cold weather [36,41–42,68–69,103–105]. While heat stimulation has most often been used for pain assessments of palmar skin in FM patients, heat hyperalgesia elicited by thermal testing of palmar skin has been detected in only a subset of FM patients, whereas cold pain hyperalgesia is more widely prevalent among FM patients, including those with heat hyperalgesia [37]. Moreover, unlike heat, cold stimulation not only elicits pain but also is more likely to be associated with dysesthesias such as “pins and needles” and paradoxical heat pain. Although the neural regulation of blood flow, especially the mechanism of vasodilation in glabrous skin, is not well understood, there is evidence that sympathetically mediated vasoconstriction of arterioles is coupled with an independent vasodilation of AVS involving CGRP and SP release from the sensory innervation under cold external conditions in order to reduce heat loss [65,91–92,97,106–108]. It is exclusively the AVS sensory innervation that appears excessive in the FM patients and may account for the increasing severity of FM symptoms under cold conditions.

Dysregulation of blood flow in the glabrous skin in humans, as a consequence of a “positive” neuropathy and AVS dysfunction, has the potential to compromise regulation of blood flow in other areas of the body. Blood flow and temperature of the skin and skeletal muscle are interdependent with inverse relationships occurring under a variety of metabolic conditions [109]. Thus, in humans, the relatively limited glabrous skin of the hands and feet and in some areas of the face and head such as the checks, nose, and ears, all specifically contain AVS, and have been shown to play a disproportionately major role in thermoregulation, given the high surface to volume ratio of these areas of the body [27,32,66,92–93,107,110–113]. Under heat stress conditions, an estimated 60% of cardiac output is distributed to the skin [66], and a particularly high proportion of this blood flow is distributed to the glabrous skin, as indicated by an estimated 6 to 1 ratio of blood flow to the palmar glabrous vs the dorsal hairy skin of the hands [95,113]. Even under moderate thermal conditions, the glabrous hand and foot skin receives a blood flow volume that far exceeds the metabolic demand, and can also withstand prolonged periods of extremely low blood flow without severe consequences. Therefore, the glabrous skin also functions as a strategic reserve that can be diverted to other tissues during transient phases of high metabolic demand. Thus, blood flow to the palms of the hands is not only reduced under cold conditions to conserve heat, but is also reduced during the onset of exercise to increase the blood supply to skeletal muscle. When prolonged exercise begins to increase core temperature, blood flow becomes rerouted especially to the glabrous skin to dissipate heat. Conceivably, the neuropathology of the AVS could result in insufficient blood flow and ischemia in deep tissues like skeletal muscles, which may contribute to the widespread deep pain and fatigue of FM, and cause compromised circadian blood flow regulation thereby impacting sleep and cognition [28,114–118].

Of potential importance to the AVS neuropathology in FM, is the particularly high occurrence of diagnosis among females, possibly pointing to a hormonal role in impacting vascular innervation, which is manifested by well-documented gender differences in normal vasoregulation [59–61,118–120]. Our data on gender differences among glabrous skin innervation in humans indicate that females normally have twice the sensory innervation to arterioles and AVS as males, whereas the sympathetic innervation is similar. Small-caliber neurovascular sensory innervation appears to be estrogen-dependent [121], which potentially underlies these gender differences and may predispose females to developing the excessive sensory innervation of the AVS observed in the FM patients. Studies are underway to determine whether a similar AVS neuropathology also occurs in male FM.

Acknowledgments

The authors wish to thank Mrs. Margaret Czerwinski, RN and Mrs. Marilyn Dockum, BS for biopsy collection and tissue processing, and Dr. Dean Kellogg for critical comments and assistance in interpreting and integrating vascular literature. The authors of this study have been funded, in part, through investigator-initiated grant support from Eli Lilly and Forest Laboratories to conduct basic research on FM. This pathology investigation is not intended to be reported to the FDA as a well-controlled human study in support of a new indication for any marketed drug, nor is this study intended to support any significant change in current FM product labeling or serve as advertising for any currently marketed drug. This research study provided strict institutional review and informed consent. The authors declare no perceived or real conflicts of interest in performing this research.

References

1 Staud R. Peripheral pain mechanisms in chronic widespread pain. Best Pract Res Clin Rheumatol 2011;25(2):155–64.

2 Vierck CJ Jr. Mechanisms underlying development of spatially distributed chronic pain (fibromyalgia). Pain 2006;124(3):242–63.

3 Wolfe F, Ross K, Anderson J, Russell IJ, Hebert L. The prevalence and characteristics of fibromyalgia in the general population. Arthritis Rheum 1995;38(1): 19–28.

4 Bradley LA. Pathophysiologic mechanisms of fibromyalgia and its related disorders. J Clin Psychiatry 2008;69(suppl 2):6–13.

5 Russell IJ, Larson AA. Neurophysiopathogenesis of fibromyalgia syndrome: A unified hypothesis. Rheum Dis Clin North Am 2009;35(2):421–35.

6 Muller W, Schneider EM, Stratz T. The classification of fibromyalgia syndrome. Rheumatol Int 2007; 27(11):1005–10.

7 Schmidt-Wilcke T, Clauw DJ. Fibromyalgia: From pathophysiology to therapy. Nat Rev Rheumatol 2011;7(9):518–27.

8 Buskila D, Sarzi-Puttini P. Biology and therapy of fibromyalgia. Genetic aspects of fibromyalgia syndrome. Arthritis Res Ther 2006;8(5):218.

9 Nilsen KB, Sand T, Westgaard RH, et al. Autonomic activation and pain in response to low-grade mental stress in fibromyalgia and shoulder/neck pain patients. Eur J Pain 2007;11(7):743–55.

10 Smith HS, Harris R, Clauw D. Fibromyalgia: An afferent processing disorder leading to a complex pain generalized syndrome. Pain Physician 2011;14(2): E217–45.

11 Arnold LM. Duloxetine and other antidepressants in the treatment of patients with fibromyalgia. Pain Med 2007;8(suppl 2):S63–74.

12 Goldenberg DL. Multidisciplinary modalities in the treatment of fibromyalgia. J Clin Psychiatry 2008; 69(suppl 2):30–4.

13 Giovengo SL, Russell IJ, Larson AA. Increased concentrations of nerve growth factor in cerebrospinal fluid of patients with fibromyalgia. J Rheumatol 1999;26(7):1564–9.

14 Larson AA, Giovengo SL, Russell IJ, Michalek JE. Changes in the concentrations of amino acids in the cerebrospinal fluid that correlate with pain in patients with fibromyalgia: Implications for nitric oxide pathways. Pain 2000;87(2):201–11.

15 Foerster BR, Petrou M, Edden RA, et al. Reduced insular gamma-aminobutyric acid in fibromyalgia. Arthritis Rheum 2012;64(2):579–83.

16 Sörensen J, Graven-Nielsen T, Henriksson KG, Bengtsson M, Arendt-Nielsen L. Hyperexcitability in fibromyalgia. J Rheumatol 1998;25(1):152–5.

17 Staud R, Koo E, Robinson ME, Price DD. Spatial summation of mechanically evoked muscle pain and painful aftersensations in normal subjects and fibromyalgia patients. Pain 2007;130(1–2):177–87.

18 Albrecht PJ, Hines S, Eisenberg E, et al. Pathologic alterations of cutaneous innervation and vasculature in affected limbs from patients with complex regional pain syndrome. Pain 2006;120(3):244–66.

19 Rice F, Albrecht P. Cutaneous mechanisms of tactile perception: Morphological and chemical organization of the innervation to the skin. In: Basbaum A, Kaneko A, eds. The Senses: A Comprehensive Reference, Vol 6, Somatosensation. San Diego: Academic Press; 2008:1–32.

20 Kennedy WR, Wendelschafer-Crabb G, Johnson T. Quantitation of epidermal nerves in diabetic neuropathy. Neurology 1996;47(4):1042–8.

21 McCarthy BG, Hsieh ST, Stocks A, et al. Cutaneous innervation in sensory neuropathies: Evaluation by skin biopsy. Neurology 1995;45(10):1848–55.

22 Oaklander AL, Romans K, Horasek S, et al. Unilateral postherpetic neuralgia is associated with bilateral sensory neuron damage. Ann Neurol 1998;44(5): 789–95.

23 Periquet MI, Novak V, Collins MP, et al. Painful sensory neuropathy: Prospective evaluation using skin biopsy. Neurology 1999;53(8):1641–7.

24 Hou Q, Barr T, Gee L, et al. Keratinocyte expression of calcitonin gene-related peptide beta: Implications for neuropathic and inflammatory pain mechanisms. Pain 2011;152(9):2036–51.

25 Petersen KL, Rice FL, Suess F, Berro M, Rowbotham MC. Relief of post-herpetic neuralgia by surgical removal of painful skin. Pain 2002;98(1–2): 119–26.

26 Zhao P, Barr TP, Hou Q, et al. Voltage-gated sodium channel expression in rat and human epidermal keratinocytes: Evidence for a role in pain. Pain 2008; 139(1):90–105.

27 Jeschonneck M, Grohmann G, Hein G, Sprott H. Abnormal microcirculation and temperature in skin above tender points in patients with fibromyalgia. Rheumatology (Oxford) 2000;39(8):917–21.

28 Katz DL, Greene L, Ali A, Faridi Z. The pain of fibromyalgia syndrome is due to muscle hypoperfusion induced by regional vasomotor dysregulation. Med Hypotheses 2007;69(3):517–25.

29 Morf S, Amann-Vesti B, Forster A, et al. Microcirculation abnormalities in patients with fibromyalgia—Measured by capillary microscopy and laser fluxmetry. Arthritis Res Ther 2005;7(2):R209–16.

30 Bradley LA. Pathophysiology of fibromyalgia. Am J Med 2009;122(suppl 12):S22–30.

31 Martinez-Lavin M. Biology and therapy of fibromyalgia. Stress, the stress response system, and fibromyalgia. Arthritis Res Ther 2007;9(4):216.

32 Reyes del Paso GA, Garrido S, Pulgar A, Duschek S. Autonomic cardiovascular control and responses to experimental pain stimulation in fibromyalgia syndrome. J Psychosom Res 2011;70(2):125–34.

33 Van Houdenhove B, Egle U, Luyten P. The role of life stress in fibromyalgia. Curr Rheumatol Rep 2005; 7(5):365–70.

34 Wolfe F, Smythe H, Yunus M, et al. The American College of Rheumatology 1990 criteria for the classification of fibromyalgia. Report of the Multicenter Criteria Committee. Arthritis Rheum 1990;33:160–72.

35 Tunks E, Crook J, Norman G, Kalaher S Tender points in fibromyalgia. Pain 1988;34(1):11–9.

36 Berglund B, Harju EL, Kosek E, Lindblom U. Quantitative and qualitative perceptual analysis of cold dysesthesia and hyperalgesia in fibromyalgia. Pain 2002;96(1–2):177–87.

37 Hurtig IM, Raak RI, Kendall SA, Gerdle B, Wahren LK. Quantitative sensory testing in fibromyalgia patients and in healthy subjects: Identification of subgroups. Clin J Pain 2001;17(4):316–22.

38 Petzke F, Clauw DJ, Ambrose K, Khine A, Gracely RH. Increased pain sensitivity in fibromyalgia: Effects of stimulus type and mode of presentation. Pain 2003;105(3):403–13.

39 Staud R, Weyl EE, Price DD, Robinson ME. Mechanical and heat hyperalgesia highly predict clinical pain intensity in patients with chronic musculoskeletal pain syndromes. J Pain 2012;13(8):725–35.

40 Staud R, Bovee CE, Robinson ME, Price DD. Cutaneous C-fiber pain abnormalities of fibromyalgia patients are specifically related to temporal summation. Pain 2008;139(2):315–23.

41 Lapossy E, Gasser P, Hrycaj P, et al. Cold-induced vasospasm in patients with fibromyalgia and chronic low back pain in comparison to healthy subjects. Clin Rheumatol 1994;13(3):442–5.

42 Kosek E, Ekholm J, Hansson P. Sensory dysfunction in fibromyalgia patients with implications for pathogenic mechanisms. Pain 1996;68(2–3):375–83.

43 Bowsher D, Geoffrey Woods C, Nicholas AK, et al. Absence of pain with hyperhidrosis: A new syndrome where vascular afferents may mediate cutaneous sensation. Pain 2009;147(1–3):287–98.

44 Eguchi S, Tezuka S, Hobara N, et al. Vanilloid receptors mediate adrenergic nerve- and CGRP-containing nerve-dependent vasodilation induced by nicotine in rat mesenteric resistance arteries. Br J Pharmacol 2004;142(7):1137–46.

45 Albrecht P, Rice F. Role of small-fiber afferents in pain mechanisms with implications on diagnosis and treatment. Curr Pain Headache Rep 2010;14(3): 179–88.

46 Fundin BT, Pfaller K, Rice FL. Different distributions of the sensory and autonomic innervation among the microvasculature of the rat mystacial pad. J Comp Neurol 1997;389(4):545–68.

47 Rice FL, Rasmusson DD. Innervation of the digit on the forepaw of the raccoon. J Comp Neurol 2000; 417(4):467–90.

48 Brain SD, Williams TJ, Tippins JR, Morris HR, MacIntyre I. Calcitonin gene-related peptide is a potent vasodilator. Nature 1985;313(5997):54–6.

49 Holzer P. Local effector functions of capsaicin-sensitive sensory nerve endings: Involvement of tachykinins, calcitonin gene-related peptide and other neuropeptides. Neuroscience 1988;24(3):739–68.

50 Holzer P. Neurogenic vasodilatation and plasma leakage in the skin. Gen Pharmacol 1998;30(1):5–11.

51 Maggi CA. Tachykinins and calcitonin gene-related peptide (CGRP) as co-transmitters released from peripheral endings of sensory nerves. Prog Neurobiol 1995;45(1):1–98.

52 Richardson JD, Vasko MR. Cellular mechanisms of neurogenic inflammation. J Pharmacol Exp Ther 2002;302(3):839–45.

53 Kruger L. The functional morphology of thin sensory axons: Some principles and problems. Prog Brain Res 1996;113:255–72.

54 Littlejohn GO, Weinstein C, Helme RD. Increased neurogenic inflammation in fibrositis syndrome. J Rheumatol 1987;14(5):1022–5.

55 Salemi S, Rethage J, Wollina U, et al. Detection of interleukin 1beta (IL-1beta), IL-6, and tumor necrosis factor-alpha in skin of patients with fibromyalgia. J Rheumatol 2003;30(1):146–50.

56 Kawasaki H, Nuki C, Saito A, Takasaki K. Adrenergic modulation of calcitonin gene-related peptide (CGRP)-containing nerve-mediated vasodilation in the rat mesenteric resistance vessel. Brain Res 1990;506(2):287–90.

57 Marvizon JC, Perez OA, Song B, et al. Calcitonin receptor-like receptor and receptor activity modifying protein 1 in the rat dorsal horn: Localization in glutamatergic presynaptic terminals containing opioids and adrenergic alpha2C receptors. Neuroscience 2007;148(1):250–65.

58 Jimenez-Mena LR, Gupta S, Munoz-Islas E, et al. Clonidine inhibits the canine external carotid vasodilatation to capsaicin by alpha2A/2C-adrenoceptors. Eur J Pharmacol 2006;543(1–3):68–76.

59 Bowyer L, Brown MA, Jones M. Vascular reactivity in men and women of reproductive age. Am J Obstet Gynecol 2001;185(1):88–96.

60 Convertino VA. Gender differences in autonomic functions associated with blood pressure regulation. Am J Physiol 1998;275(6 Pt 2):R1909–20.

61 Cooke JP, Creager MA, Osmundson PJ, Shepherd JT. Sex differences in control of cutaneous blood flow. Circulation 1990;82(5):1607–15.

62 Pare M, Albrecht PJ, Noto CJ, et al. Differential hypertrophy and atrophy among all types of cutaneous innervation in the glabrous skin of the monkey hand during aging and naturally occurring type 2 diabetes. J Comp Neurol 2007;501(4):543–67.

63 Uceyler N, Zeller D, Kahn AK, et al. Small fibre pathology in patients with fibromyalgia syndrome. Brain 2013. doi: 10.1093/brain/awt053.

64 Oaklander AL. The density of remaining nerve endings in human skin with and without postherpetic neuralgia after shingles. Pain 2001;92(1–2):139–45.

65 Grant RT, Bland EF. Observations on arteriovenous anastomoses in human skin and the bird's foot with special reference to reaction to cold. Heart 1931; 15:381–411.

66 Burton AC. The range and variability of the blood flow in the human fingers and the vasomotor regulation of body temperature. Am J Physiol 1939;127:437–53.

67 Petersen KL, Rice FL, Farhadi M, Reda H, Rowbotham MC. Natural history of cutaneous innervation following herpes zoster. Pain 2010;150(1):75–82.

68 Friend R, Bennett RM. Distinguishing fibromyalgia from rheumatoid arthritis and systemic lupus in clinical questionnaires: An analysis of the revised Fibromyalgia Impact Questionnaire (FIQR) and its variant, the Symptom Impact Questionnaire (SIQR), along with pain locations. Arthritis Res Ther 2011;13(2):R58.

69 Guedj D, Weinberger A. Effect of weather conditions on rheumatic patients. Ann Rheum Dis 1990; 49(3):158–9.

70 Kalliomaki M, Kieseritzky JV, Schmidt R, et al. Structural and functional differences between neuropathy with and without pain? Exp Neurol 2011;231(2):199–206.

71 Simms RW, Goldenberg DL, Felson DT, Mason JH. Tenderness in 75 anatomic sites. Distinguishing fibromyalgia patients from controls. Arthritis Rheum 1988;31(2):182–7.

72 Arroyo JF, Cohen ML. Abnormal responses to electrocutaneous stimulation in fibromyalgia. J Rheumatol 1993;20(11):1925–31.

73 Kosek E, Ekholm J, Hansson P. Increased pressure pain sensibility in fibromyalgia patients is located deep to the skin but not restricted to muscle tissue. Pain 1995;63(3):335–9.

74 Staud R, Craggs JG, Perlstein WM, Robinson ME, Price DD. Brain activity associated with slow temporal summation of C-fiber evoked pain in fibromyalgia patients and healthy controls. Eur J Pain 2008; 12(8):1078–89.

75 Staud R, Robinson ME, Price DD. Temporal summation of second pain and its maintenance are useful for characterizing widespread central sensitization of fibromyalgia patients. J Pain 2007;8(11):893–901.

76 DeSantana JM, Sluka KA. Central mechanisms in the maintenance of chronic widespread noninflammatory muscle pain. Curr Pain Headache Rep 2008; 12(5):338–43.

77 Reyes Del Paso GA, Pulgar A, Duschek S, Garrido S. Cognitive impairment in fibromyalgia syndrome: The impact of cardiovascular regulation, pain, emotional disorders and medication. Eur J Pain 2012;16(3): 421–9.

78 Barohn RJ. Intraepidermal nerve fiber assessment: A new window on peripheral neuropathy. Arch Neurol 1998;55(12):1505–6.

79 Beiswenger KK, Calcutt NA, Mizisin AP. Epidermal nerve fiber quantification in the assessment of

diabetic neuropathy. Acta Histochem 2008;110(5): 351–62.

80 Lauria G, Lombardi R, Camozzi F, Devigili G. Skin biopsy for the diagnosis of peripheral neuropathy. Histopathology 2009;54(3):273–85.

81 Barr TP, Albrecht PJ, Hou Q, et al. Air-stimulated ATP release from keratinocytes occurs through connexin hemichannels. PloS ONE 2013;8(2):e56744.

82 Dussor G, Koerber HR, Oaklander AL, Rice FL, Molliver DC. Nucleotide signaling and cutaneous mechanisms of pain transduction. Brain Res Rev 2009; 60(1):24–35.

83 Donadio V, Nolano M, Provitera V, et al. Skin sympathetic adrenergic innervation: An immunofluorescence confocal study. Ann Neurol 2006;59(2): 376–81.

84 Cannon KE, Chazot PL, Hann V, et al. Immunohistochemical localization of histamine H3 receptors in rodent skin, dorsal root ganglia, superior cervical ganglia, and spinal cord: Potential antinociceptive targets. Pain 2007;129(1–2):76–92.

85 Molliver DC, Immke DC, Fierro L, et al. ASIC3, an acid-sensing ion channel, is expressed in metaboreceptive sensory neurons. Mol Pain 2005;1:35.

86 Burnstock G, Ralevic V. New insights into the local regulation of blood flow by perivascular nerves and endothelium. Br J Plast Surg 1994;47(8):527–43.

87 Lundberg JM, Rudehill A, Sollevi A, Theodorsson-Norheim E, Hamberger B. Frequency- and reserpine-dependent chemical coding of sympathetic transmission: Differential release of noradrenaline and neuropeptide Y from pig spleen. Neurosci Lett 1986;63(1):96–100.

88 Stjarne L. Basic mechanisms and local modulation of nerve impulse-induced secretion of neurotransmitters from individual sympathetic nerve varicosities. Rev Physiol Biochem Pharmacol 1989;112:1–137.

89 Johnson JM, Pergola PE, Liao FK, Kellogg DL Jr, Crandall CG. Skin of the dorsal aspect of human hands and fingers possesses an active vasodilator system. J Appl Physiol 1995;78(3):948–54.

90 Hales JR, Jessen C, Fawcett AA, King RB. Skin AVA and capillary dilatation and constriction induced by local skin heating. Pflugers Arch 1985;404(3):203–7.

91 Holzer P. Peptidergic sensory neurons in the control of vascular functions: Mechanisms and significance in the cutaneous and splanchnic vascular beds. Rev Physiol Biochem Pharmacol 1992;121:49–146.

92 Johnson JM, Kellogg DL Jr. Local thermal control of the human cutaneous circulation. J Appl Physiol 2010;109(4):1229–38.

93 Kellogg DL, Jr. In vivo mechanisms of cutaneous vasodilation and vasoconstriction in humans during thermoregulatory challenges. J Appl Physiol 2006; 100(5):1709–18.

94 Magerl W, Treede RD. Heat-evoked vasodilatation in human hairy skin: Axon reflexes due to low-level activity of nociceptive afferents. J Physiol 1996; 497:(Pt 3):837–48.

95 Metzler-Wilson K, Kellie LA, Tomc C, et al. Differential vasodilatory responses to local heating in facial, glabrous and hairy skin. Clin Physiol Funct Imaging 2012;32(5):361–6.

96 Yamada M, Ishikawa T, Fujimori A, Goto K. Local neurogenic regulation of rat hindlimb circulation: Role of calcitonin gene-related peptide in vasodilatation after skeletal muscle contraction. Br J Pharmacol 1997;122(4):703–9.

97 Charkoudian N. Mechanisms and modifiers of reflex induced cutaneous vasodilation and vasoconstriction in humans. J Appl Physiol 2010;109(4):1221–8.

98 Schini-Kerth VB, Fisslthaler B, Busse R. CGRP enhances induction of NO synthase in vascular smooth muscle cells via a cAMP-dependent mechanism. Am J Physiol 1994;267(6 Pt 2):H2483–90.

99 Ballet S, Aubel B, Mauborgne A, et al. The novel analgesic, cizolirtine, inhibits the spinal release of substance P and CGRP in rats. Neuropharmacology 2001;40(4):578–89.

100 Chotani MA, Flavahan S, Mitra S, Daunt D, Flavahan NA. Silent alpha(2C)-adrenergic receptors enable cold-induced vasoconstriction in cutaneous arteries. Am J Physiol Heart Circ Physiol 2000;278(4):H1075–83.

101 Kawasaki H, Nuki C, Saito A, Takasaki K. NPY modulates neurotransmission of CGRP-containing vasodilator nerves in rat mesenteric arteries. Am J Physiol 1991;261(3 Pt 2):H683–90.

102 Russell IJ, Orr MD, Littman B, et al. Elevated cerebrospinal fluid levels of substance P in patients with the fibromyalgia syndrome. Arthritis Rheum 1994; 37(11):1593–601.

103 Bennett RM, Clark SR, Campbell SM, et al. Symptoms of Raynaud's syndrome in patients with fibromyalgia. A study utilizing the Nielsen test, digital photoplethysmography, and measurements of

platel*et* *al*pha 2-adrenergic receptors. Arthritis Rheum 1991;34(3):264–9.

104 Lautenbacher S, Rollman GB, McCain GA. Multimethod assessment of experimental and clinical pain in patients with fibromyalgia. Pain 1994;59(1):45–53.

105 Macfarlane TV, McBeth J, Jones GT, Nicholl B, Macfarlane GJ. Whether the weather influences pain? Results from the EpiFunD study in North West England. Rheumatology (Oxford) 2010;49(8):1513–20.

106 Minson CT. Thermal provocation to evaluate microvascular reactivity in human skin. J Appl Physiol 2010;109(4):1239–46.

107 Bergersen TK, Hisdal J, Walloe L. Perfusion of the human finger during cold-induced vasodilatation. Am J Physiol 1999;276(3 Pt 2):R731–7.

108 Hodges GJ, Traeger JA 3rd, Tang T, et al. Role of sensory nerves in the cutaneous vasoconstrictor response to local cooling in humans. Am J Physiol Heart Circ Physiol 2007;293(1):H784–9.

109 Friedlander M, Silbert S, Bierman W, Laskey N. Differences in temperature of skin and muscles of the lower extremities following various procedures. Proc Soc Exp Biol Med 1938;38:150.

110 Bergersen TK, Eriksen M, Walloe L. Local constriction of arteriovenous anastomoses in the cooled finger. Am J Physiol 1997;273(3 Pt 2):R880–6.

111 Johnson JM, Yen TC, Zhao K, Kosiba WA. Sympathetic, sensory, and nonneuronal contributions to the cutaneous vasoconstrictor response to local cooling. Am J Physiol Heart Circ Physiol 2005;288(4):H1573–9.

112 Vanggaard L, Kuklane K, Holmer I, Smolander J. Thermal responses to whole-body cooling in air with special reference to arteriovenous anastomoses in fingers. Clin Physiol Funct Imaging 2012;32(6):463–9.

113 Wilson TE, Zhang R, Levine BD, Crandall CG. Dynamic autoregulation of cutaneous circulation: Differential control in glabrous versus nonglabrous skin. Am J Physiol Heart Circ Physiol 2005;289(1):H385–91.

114 Elvin A, Siosteen AK, Nilsson A, Kosek E. Decreased muscle blood flow in fibromyalgia patients during standardised muscle exercise: A contrast media enhanced colour Doppler study. Eur J Pain 2006;10(2):137–44.

115 Furlan R, Colombo S, Perego F, et al. Abnormalities of cardiovascular neural control and reduced orthostatic tolerance in patients with primary fibromyalgia. J Rheumatol 2005;32(9):1787–93.

116 Kasikcioglu E, Dinler M, Berker E. Reduced tolerance of exercise in fibromyalgia may be a consequence of impaired microcirculation initiated by deficient action of nitric oxide. Med Hypotheses 2006;66(5):950–2.

117 Lund N, Bengtsson A, Thorborg P. Muscle tissue oxygen pressure in primary fibromyalgia. Scand J Rheumatol 1986;15(2):165–73.

118 Marchand I, Johnson D, Montgomery D, Brisson GR, Perrault H. Gender differences in temperature and vascular characteristics during exercise recovery. Can J Appl Physiol 2001;26(5):425–41.

119 Bartelink ML, Wollersheim H, Theeuwes A, van Duren D, Thien T. Changes in skin blood flow during the menstrual cycle: The influence of the menstrual cycle on the peripheral circulation in healthy female volunteers. Clin Sci (Lond) 1990;78(5):527–32.

120 Evans JM, Ziegler MG, Patwardhan AR, et al. Gender differences in autonomic cardiovascular regulation: Spectral, hormonal, and hemodynamic indexes. J Appl Physiol 2001;91(6):2611–8.

121 Blacklock AD, Cauveren JA, Smith PG. Estrogen selectively increases sensory nociceptor innervation of arterioles in the female rat. Brain Res 2004;1018(1):55–65.